

**MHz Class Repetitively Q-Switched, High-Power Ruby Lasers for High-Speed
Photographic Applications**

Peter E. Nebolsine
Physical Sciences Inc.
20 New England Business Center
Andover, MA 01810

D. R. Snyder
Air Force Research Laboratory
Eglin AFB, FL 32542

J. M. Grace
Cambridge, MA 02139

AIAA 2001-0845
39th AIAA Aerospace Sciences Meeting
8-11 January 2001, Reno, NV

IN-HOUSE COVER

Report Documentation Page				Form Approved OMB No. 0704-0188	
Public reporting burden for the collection of information is estimated to average 1 hour per response, including the time for reviewing instructions, searching existing data sources, gathering and maintaining the data needed, and completing and reviewing the collection of information. Send comments regarding this burden estimate or any other aspect of this collection of information, including suggestions for reducing this burden, to Washington Headquarters Services, Directorate for Information Operations and Reports, 1215 Jefferson Davis Highway, Suite 1204, Arlington VA 22202-4302. Respondents should be aware that notwithstanding any other provision of law, no person shall be subject to a penalty for failing to comply with a collection of information if it does not display a currently valid OMB control number.					
1. REPORT DATE JAN 2001		2. REPORT TYPE		3. DATES COVERED 00-00-2001 to 00-00-2001	
4. TITLE AND SUBTITLE MHz Class Repetitively Q-Switched, High-Power Ruby Lasers for High-Speed Photographic Applications				5a. CONTRACT NUMBER	
				5b. GRANT NUMBER	
				5c. PROGRAM ELEMENT NUMBER	
6. AUTHOR(S)				5d. PROJECT NUMBER	
				5e. TASK NUMBER	
				5f. WORK UNIT NUMBER	
7. PERFORMING ORGANIZATION NAME(S) AND ADDRESS(ES) Physical Sciences Inc,20 New England Business Center,Andover,MA,01810				8. PERFORMING ORGANIZATION REPORT NUMBER	
9. SPONSORING/MONITORING AGENCY NAME(S) AND ADDRESS(ES)				10. SPONSOR/MONITOR'S ACRONYM(S)	
				11. SPONSOR/MONITOR'S REPORT NUMBER(S)	
12. DISTRIBUTION/AVAILABILITY STATEMENT Approved for public release; distribution unlimited					
13. SUPPLEMENTARY NOTES					
14. ABSTRACT see report					
15. SUBJECT TERMS					
16. SECURITY CLASSIFICATION OF:			17. LIMITATION OF ABSTRACT Same as Report (SAR)	18. NUMBER OF PAGES 13	19a. NAME OF RESPONSIBLE PERSON
a. REPORT unclassified	b. ABSTRACT unclassified	c. THIS PAGE unclassified			



AIAA 2001-0845

MHz Class Repetitively Q-Switched, High-Power Ruby Lasers for High-Speed Photographic Applications

Peter E. Nebolsine
Physical Sciences Inc.
20 New England Business Center
Andover, MA 01810

D. R. Snyder
Air Force Research Laboratory
Eglin AFB, FL 32542

J. M. Grace
Cambridge, MA 02139

**39th AIAA Aerospace Sciences
Meeting & Exhibit**
8-11 January 2001 / Reno, Nevada

MHZ CLASS REPETITIVELY Q-SWITCHED, HIGH-POWER RUBY LASERS FOR HIGH-SPEED PHOTOGRAPHIC APPLICATIONS

P.E. Nebolsine*
Physical Sciences Inc.
Andover, MA 01810

D. R. Snyder#
Air Force Research Laboratory
Eglin AFB, FL 32542

J. M. Grace\$
Cambridge, MA 02139

Abstract

Repetitively pulsed lasers have been developed that have served as excellent illumination sources for high speed framing photography. This invited paper discusses the general subject of laser illuminators for high speed photography as well as specific capabilities of a high repetition rate Q switched ruby laser system that provides laser pulse repetition rates up to 1 MHz. Individual laser pulse energies of ~ 1 J are obtained at a laser repetition rate of 250 kHz, and proportionately lower energies as the pulse repetition rate is increased to 1 MHz. Nearly uniform pulse to pulse micropulse laser pulse energies are obtained providing for nearly constant illumination over the ~ 120 μ s laser pulse envelope duration. Example images are provided illustrating the integration of the ruby laser system and camera system with a gun range to obtain high speed framing camera images of ballistic events.

Introduction

Repetitively pulsed lasers have been developed that have served as excellent illumination sources for high speed framing photography. The key attributes that repetitively pulsed lasers provide include: sufficient energy per pulse to provide the necessary illumination for image capture, short pulse time duration to “freeze”

the motion of a high speed event, and controllable pulse timing to provide proper laser synchronization with the event and camera. Also, in some cases the added feature of the laser’s spectrally narrow optical emission coupled with the use of a narrow passband filter at the camera’s entrance aperture allows image capture using the laser’s illumination while excluding a high fraction of broadband confounding luminosity associated with a self luminous event. This invited paper discusses the general subject of laser illuminators for high speed photography as well as specific capabilities of a high repetition rate Q switched ruby laser system that provides laser pulse repetition rates up to 1 MHz.

Since the required laser energy per pulse can be substantial, several different approaches have been used by different investigators when assembling a laser system to meet their needs. Q-switching is universally used to generate a short temporal duration pulse yet high peak power with sufficient laser energy per pulse for successful implementation. Reference 1 contains a discussion of Q-switching, a method to obtain a pulse or pulses from a laser medium that can store energy in the population inversion and generate an optical pulse with a peak power far greater than the power used to pump the laser rod. The laser pulse time is short, typically 5 to 10’s ns pulse length, and the peak power is high, resulting in single pulse output energies of ~ 1 μ J to ~ 1 J output energy per pulse. Typically using a ruby laser with the output wavelength of 694 nm, or frequency doubling the output of a Nd:YAG (output wavelength of 1064 nm) is done to provide illumination at wavelengths where photographic film or solid state CCD cameras are sensitive.

Some investigators have used a “Gatling Gun” type arrangement of individual lasers to obtain significant energy per pulse and short times between pulses, e.g., high repetition rate. Shaw et al. is an

*Physical Sciences Inc., Andover, MA 01810,
nebolsine@psicorp.com, Member AIAA

#Air Force Research Laboratory, Eglin AFB, FL 32542

\$Independent consultant, Cambridge, MA 02139

example of a custom ruby laser system, $\lambda = 694$ nm, that combines the capability of using four separate regions of a ruby rod for separate Q-switched laser cavities as well as to have two of these units to form a pulse train of up to eight pulses.²⁻³ Francis on the other hand, used four commercially available frequency doubled Nd:YAG lasers, $\lambda = 532$ nm, each with a single or double pulse output waveform.⁴ The use of multiple independently triggered lasers does provide enhanced timing flexibility, i.e., to obtain pulse repetition rates in excess of 1 MHz. However, events associated with impacts and the detonation of explosives do not require framing rates in excess of 1 MHz. Hence, a high repetition rate Q-switch applied to a single laser cavity an attractive alternative, particularly when greater than ten pulses are required. This approach for ruby lasers is described in References 5 to 11. It is this approach that is the principal subject of this invited paper. Alternatively, chopping the output of a CW Nd:YAG laser, using external high speed Pockels cells and then frequency doubling to 532 nm has been applied to supersonic flow visualization.¹² Alternatively, repetitively Q-switching Nd:YAG laser is commercially available, though at lower pulse repetition rates.

System Description

The imaging system described herein consists of an integrated ruby laser and CCD camera. High-speed images of ballistic impact events were acquired. The following sections briefly describe the laser and camera. The experimental imaging setup is then presented along with the results of the successful integration. This paper concludes with a description of the integration timing diagrams.

2.1 Ruby Laser

Q-switching of a laser cavity is normally done once to obtain a single giant pulse. This is usually done near the end of the flashlamp pump when the population inversion in the rod is at its highest. To obtain multiple pulses, the laser cavity is repetitively Q-switched over a period of time for which the gain is greater than the losses associated with the laser cavity. It has been found that the laser cavity can be repetitively Q-switched with resulting pulses formed, for approximately the same duration in which the laser will emit when free running (normal mode operation).

A two stage amplification repetitively Q-switched ruby laser was developed by Physical Sciences Inc. (PSI) in partnership with Continuum Electro-Optics Inc. under the Small Business Innovative Research program with the Air Force Research Laboratory (AFRL/MNMF). The oscillator stage incorporates the multiple

Q-switching intracavity technology followed by two amplification stages. The current version of this laser uses two amplification stages and a novel pulse envelope former to maintain nearly uniform pulse to pulse energy stability within the macropulse envelope.

As an example of the laser performance, Figures 1 and 2 show the photodetector traces and energy per pulse results for pulse repetition frequencies (PRF's) at 500 and 250 kHz, respectively. These figures exhibit nearly ideal pulse-to-pulse stability. Figures 1a, 1b, 2a, and 2b were again acquired using a load resistor to integrate the photodetector response. An active optical

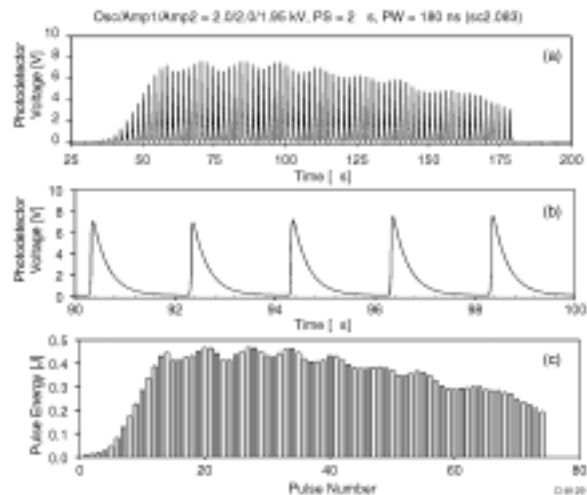


Figure 1. A 500 kHz pulse train with total energy = 24.9 J: (a) macropulse envelope, (b) expanded time scale of (a), and (c) energy per pulse in (a).

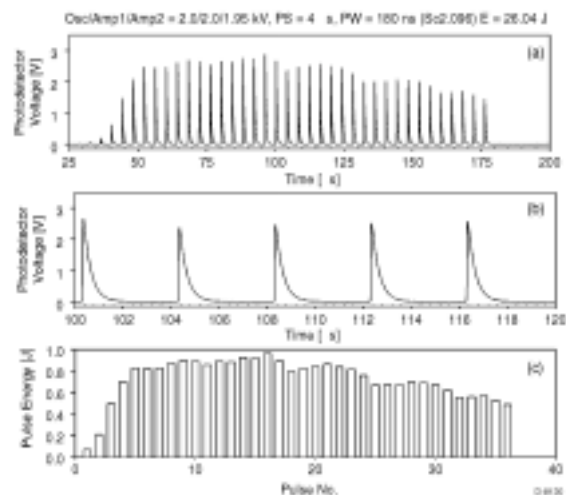


Figure 2. A 250 kHz pulse train with total energy = 26.0 J: (a) macropulse envelope, (b) expanded time scale of (a), and (c) energy per pulse in (a).

element placed between the oscillator cavity and first amplification stage artificially terminated the macropulse. This element shaped the macropulse envelope to achieve even better stability. The macropulse duration was designed to ensure the laser produces tens of pulses per shot.

Figures 1 and 2 show that the individual pulse energies are of the order of 350 mJ for 500 kHz laser pulse repetition rate and more than double that to a peak of nearly 1 J/pulse at 250 kHz. Pulse energy scales inversely with PRF for this operational envelope of the laser, as seen in Figure 3. This figure shows the macropulse energy as a function of PRF for two pump energies of amplifier stage 1 (2900 and 3600 J) and a fixed pump energy of the oscillator cavity (3600 J). This operational envelope is clearly below saturation, indicating that even higher pulse energies can be obtained. The optical gain for these amplification stages is roughly X25 for stage 1 and X2 for stage 2. Stage 1 is a double-passed amplifier and most of the gain (~ X9) occurs on the first pass, which the second pass is about X2.5. Since the ruby rods in the oscillator and the amplifier stage 1 are the same size, clearly the oscillator does not operate at maximum energy extraction.

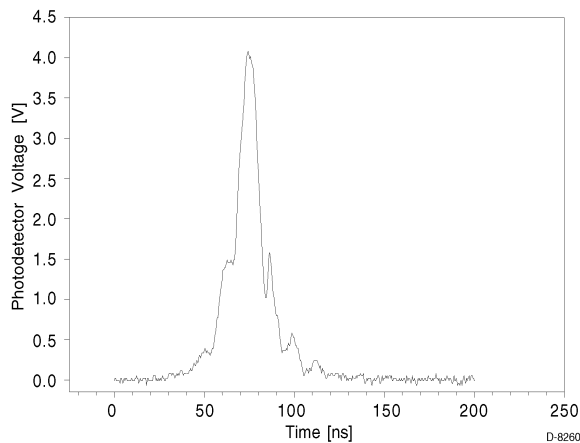


Figure 3. Total macropulse energy for 500 and 250 kHz at a fixed oscillator pump energy and two stage 1 amplifier pump energies.

Figure 4 shows a single laser pulse trace isolated from the center region of a macropulse fired with the settings of Figure 2 (250 kHz). This method uses the full bandwidth of the detector and oscilloscope. The FWHM of this laser pulse is approximately 10 ns (however, 75% of the energy is delivered in approximately 25 ns). This fact pulse length coupled with the low jitter due to the fact that the pulse forms near the close of the Pockels cell yields a highly

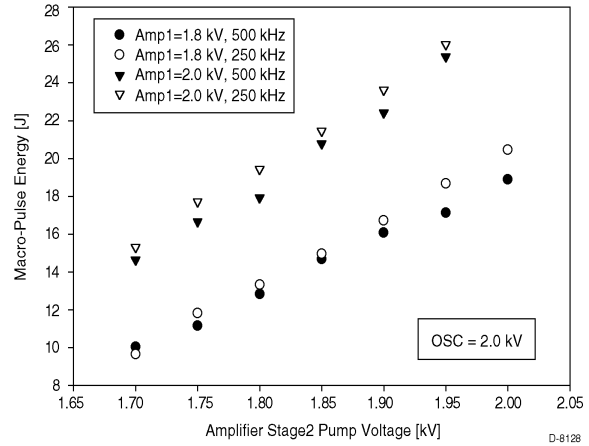


Figure 4. Fast time response trace of a single pulse from 250 kHz data.

desirable combination for stop motion photography. In essence, motion is frozen regardless of the open shutter time because the illumination is restricted to such a short laser pulse duration (e.g., an object moving at 5 km/s travels 50 μm in 10 ns).

2.2 Camera

Silicon Mountain Design Inc., now DALSA, developed the camera used here. The SMD-64k1M camera is capable of imaging 1,000,000 frames per second using a 256 X 256 array with the ability to store 17 frames with true 12 bits of dynamic range. (16 frames are normally used for data and one for the active or open frame. With normal illumination this frame is open during readout and integrates ambient light until the mechanical shutter closes. With laser strobe this 17th frame becomes useful for data, or in a number of configurations a final still frame with multiple exposures from laser pulses.) This camera allows researchers to capture multiple high-speed events using solid state technology housed in a 53 in.³ package.

The SMD-64k1M, so named by virtue of 64 k pixels operating at 1 Million frames per second, uses a proprietary CCD architecture allowing up to 16 frames to be stored on the CCD, which can be read out at a later time. The camera (shown in Figure 5) is housed in an enclosure measuring 4 in. on each side, to which a C mount lens can be attached.

The basic CCD is a 1K by 1K frame transfer array with custom timing and a metallic aperture mask applied by SMD to define the active pixels and storage registers. A stairstep pattern of the CCD mask is implemented that results in an output image roll of 14°.



Figure 5. SMD64k1M Million Frame per Second Camera.

This is compensated in the test set up with a wedge in the camera mount. Once the memory is filled the image sequence is read out of 4 on chip amplifiers at 20 Mpixels/sec. In this way, the 64k1M can be readout in 16 ms, or at 60 sequences per second. Thus, after acquiring 16 frames at 1 million frames per second, the camera can be ready to acquire another 16 frames in 16 ms. The resulting 12 bit files can be viewed a composite sheet as the figures in the paper, a movie file, or individual 12 bit TIFF files.

Experimental Setup

Typical applications for high speed imaging systems require large area illumination, on the order of 1000 cm^2 . Diffusers are also incorporated to remove laser speckle from the image. A low power negative lens and ground glass diffuser were incorporated into the optical train as shown in the following figure. Here the beam exiting the laser room has approximately a 1 in. diameter. The resulting illumination area on the target is on the order of 2500 cm^2 . Most exposures

were acquired with a target to camera distance of about 4 m. Tokina 35mm (150 to 500mm) zoom lens (f5.6/f32) were used on the cameras. Field of view varied from 250 mm to 75 mm. Most exposures were made at f/11 to f/16. Provision for filtering ambient light with ruby laser line filters and neutral density filters from Andover Optics was made. The ruby line filters were also used to reject light from the impact flash during tests with metal objects. Speckle was controlled using lens tissue sandwiched between two layers of 3 mm thick ground glass. Later tests made use of a holographic polymer diffusers from Physical Optics Corporation. A high light transmission (over 90%) was obtained.

The laser pulse energy was selected based on the sensitivity of the CCD array and imaging geometry. The SMD64k1M has a full well capacity of 213,000 electrons with a quantum efficiency on the order of 10%. These numbers coupled with the desired exposure level of 50% full well depth dictated micropulse energy on the order of 100 mJ/pulse (approximately 7 J/macropulse). The calculation method is explained in more detail in Reference 9. Using a calibration figure similar to Figure 3 the flashlamp voltages were selected to deliver the required pulse energy.

The light gate for triggering consisted of two OPOS Electronics EV120 infrared trigger screens. The unit projects a thin line of IR light using IR light emitting diodes. The two IR screens were mounted in a timing tube arrangement two feet apart. The signal generated by the passing projectile started a counter in a Cordin Model 463 Proportional Delay trigger unit. This unique device measures the velocity of the projectile and provides a delayed output to the laser and cameras

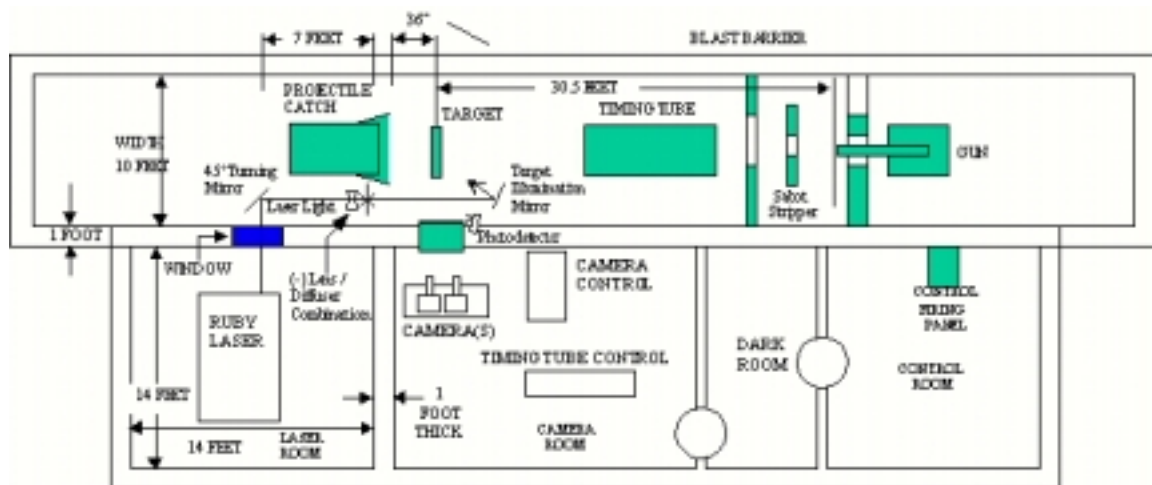


Figure 6. Experimental setup at Bay-10 showing positions of laser, camera, target launcher and range control. Schematic also shows the optical setup to direct laser light onto target.

based on a user-entered multiplier. The multiplier delays the trigger output to account for the time between light gate and target as well as laser firing delays. In the laser/camera master/slave trigger sequence, the laser trigger was buffered using a Stanford Research Systems (DG535) delay generator. The delay generator provided additional timing control as well as further electronic isolation of the camera trigger circuit from the laser noise.

The following two figures illustrate the integrated imaging system. These images were acquired in real-time with the laser and CCD camera coupled to the range master clock. Here the test object was plate glass approximately 3 mm thick. A NATO 7.62 round fired from the gun tube upstream impacted the glass near the center of the image plane. (Note that the NATO 7.62 x 51 mm round is equivalent to the .308 Winchester sporting round).

The projectile in these images travels at approximately 840 m/s with a kinetic energy of approximately 3270 J. The fragment field resulting from the impact as well as crack propagation cannot readily be resolved in Figure 7. This deficiency is not inherent to the imaging system, rather a characteristic of the 'proof of concept' nature of these tests. The projectile speed limits the amount of information available in this impact scenario as the bullet travels only 1.7 mm in 2 μ s. Hence from frame to frame the bullet travels only 8% of its overall length, and during the full exposure time 1.4X its length. Such a 'slow and large' object does not fully take advantage of the high-speed capability of the imaging system. The benefits of a high framing rate apply to objects moving on the order of their characteristic dimension per frame. The imaging configuration must be selected to yield sufficient field of view with appropriate resolution. The imaging configuration used for the tests described in Figures 7,8 was not designed to resolve mm size fragments.

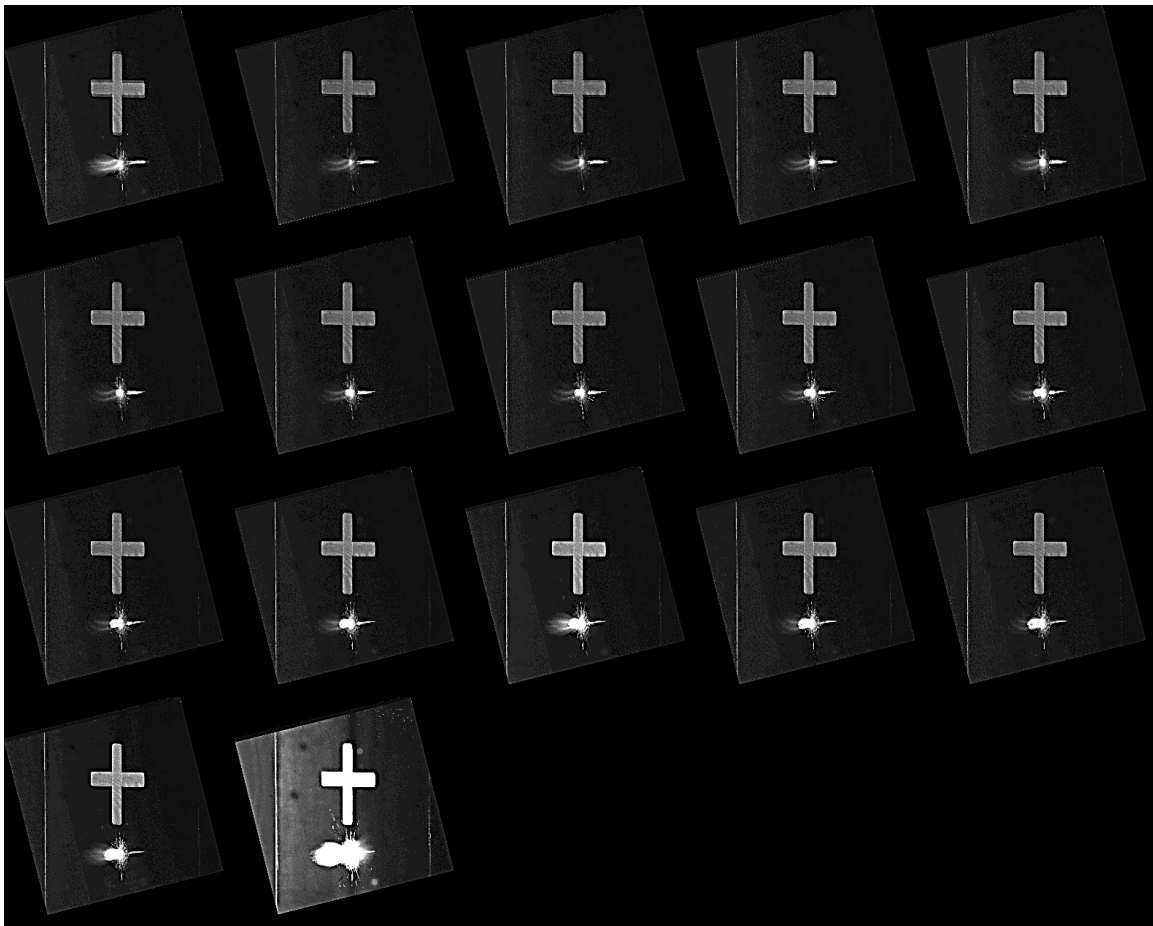


Figure 7. Ballistic impact images acquired in real-time using laser and camera at 500 kHz. The test object is plate glass approximately 3 mm thick and the projectile is a NATO 7.62 round. Bullet travels from right to left.



Figure 8. Ballistic impact images acquired in real-time using laser and camera at 250 kHz. The test object is plate glass approximately 3 mm thick and the projectile is a NATO 7.62 round. Bullet travels from right to left.

A better use of the laser and camera for imaging the impact zone of a NATO 7.62 round is at 250 kHz. Figure 8 demonstrates the slower speed imaging capability. Here again, a NATO 7.62 round is fired into plate glass and the impact zone including the fragment field is readily observed. Since the laser pulse provides the only illumination, the stop action feature of this imaging system is effectively on the order of 40 MHz, regardless of the camera integration time (2.7 μ s at 250 kHz).

Another capability of the imaging system not presented in this paper is that the CCD camera allows multiple gating of the 16 frames, e.g., n frames can be timed to an initial event (e.g., launch of an EFP), and the remaining frames timed to the final event (impact). The laser is not currently configured to accept multiple gating, though the pulse train emitted does cover a significant portion of a high speed event (150 μ s).

A modification to the CCD mask was made following the above tests. This modification reduced cross-talk and allowed for higher quality image acquisition. The following three figures (Figures 9, 10, and 11) present images acquired with the camera and laser at the Bay-10 gun range. Due to the slow projectile speed, the image acquisition system was slowed down to 125-250 kHz. Additionally, the imaging configuration was selected to increase the resolution beyond that of Figures 7 and 8.

Integration Timing Diagrams

Recent advances in the trigger circuitry of the CCD camera allowed precise synchronization of the laser pulses and camera's open shutter times. Previously, both systems utilized state-triggers with one microsecond intermittence (i.e., uncertainty). Such an uncertainty required running the laser and camera asynchronously to ensure laser exposure of at least some of the frames in the image window.¹⁰ Modifications to the CCD circuitry reduced the

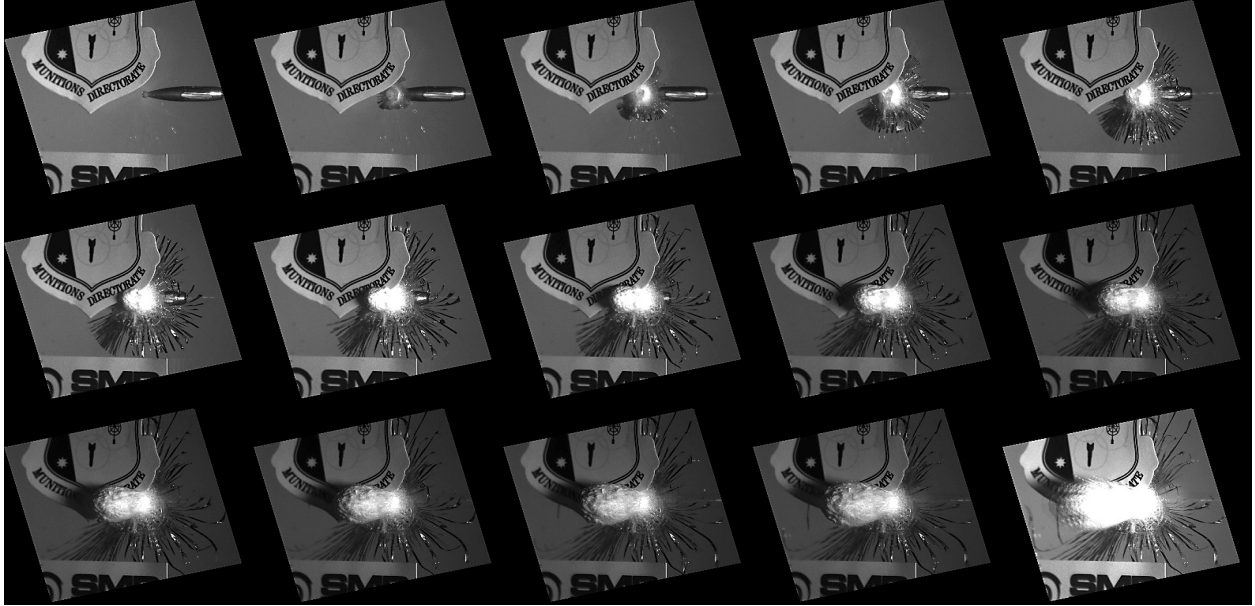


Figure 9: Projectile impact on a 3 mm thick plate glass. (7.62 mm bullet imaged at 125 kHz).



Figure 10: Projectile impact on a water bottle. Image shows the formation of a shock wave and bubble field. (7.62 mm bullet imaged at 125 kHz)

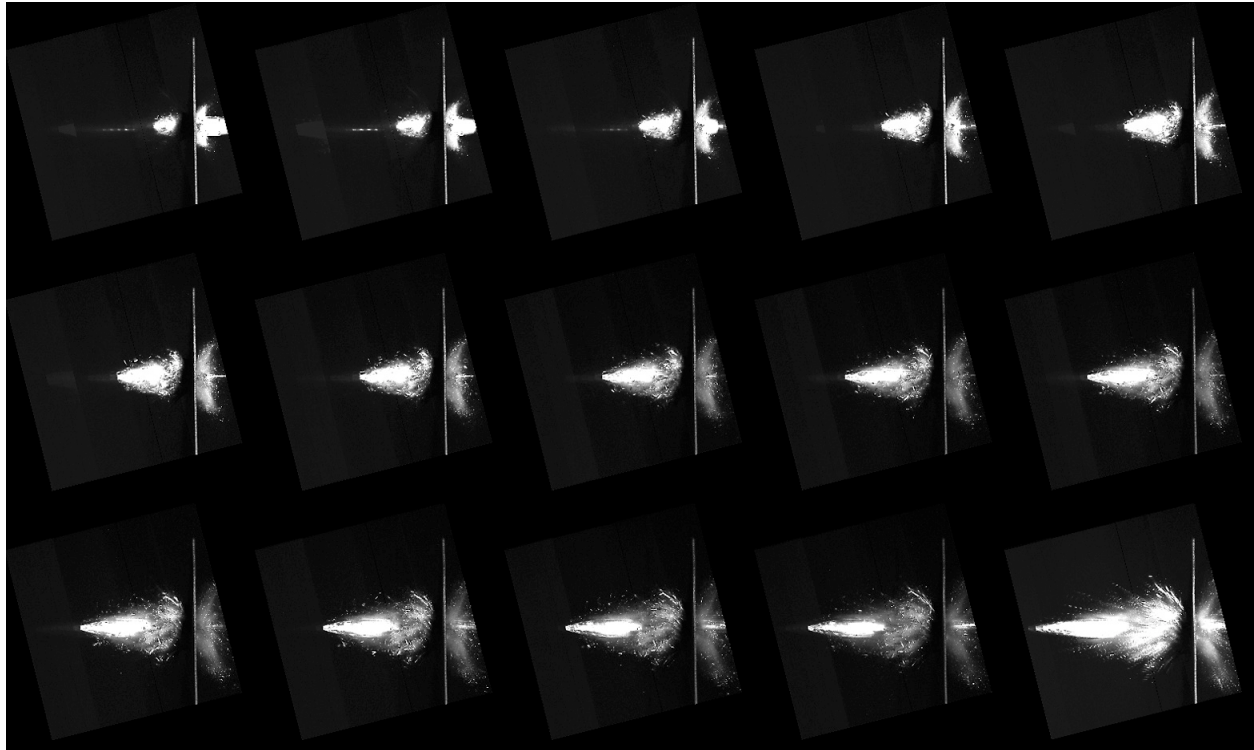


Figure 11: Projectile impact on a thin composite (side view). (7.62 mm bullet imaged at 125 kHz).

uncertainty down to 50 ns. Given an integration time on the order of 700 ns for 500 kHz operation, this jitter is trivial. The range clock controls the master time for all tests. Therefore, to integrate the imaging system into the gun range, the imaging system must be slaved to the range. It is a detail to note that the laser is slaved directly to the range master clock and the camera is then slaved to the laser.

Range safety requirements dictate evacuation of the laser room and gun tunnel prior to a test. Therefore, the laser must be controlled remotely. A remote charge and fire circuit (along with a remote capacitor dump) makes this possible. Characteristically, solid-state, flashlamp-pumped lasers require a significant and imprecise charging laser rod pumping times and followed with laser emission only after the gain=loss threshold has been reached. This does not hinder remote operation or the precise timing of the laser output. Due to the high precision and accuracy with which the laser pulses must be located relative to the projectile path, the charging of the capacitors is done "out of the loop." That is, the capacitors are charged before the fire sequence. A refresh circuit on the laser capacitor banks assures that the capacitors remain charged indefinitely (the remote dump provides proper safety). Once the laser receives the "fire" trigger, the flashlamps fire and a pulse train is

emitted after the laser reaches threshold. Just prior to threshold, the laser control unit triggers the start of the sequencing of the high speed Pockels cell that provides for the repetitive Q-switching and precisely locates the laser pulses in time. The CCD camera(s) is then slaved to this high speed Pockels cell resulting in synchronization of the laser pulse and the CCD integration time. Figure 12 shows a scope trace taken during the shot in Figure 7. Here the laser pulses measured by the photodetector and the integration gate pulses generated by the camera overlap, clearly demonstrating synchronization. The precision of this sequence is such that the laser pulse can be moved at will to any part of the integration window. Details of the fire sequence follow in Figures 13 and 14.

Figure 13 presents a timing diagram describing the sequence of events in the test. Note that the time axis (horizontal) is not to scale. The time markers are labeled at the bottom of the figure. Here a negative subscript indicates that the range safety officer controls the timing of the test. Positive subscripts indicate that the range master clock has control of the test. Time zero is defined when the projectile trips the first light gate. The delay from t_0 to t_1 is a calibrated delay taking into account the target time (i.e., the distance from the light gate to the target divided by the projectile speed)

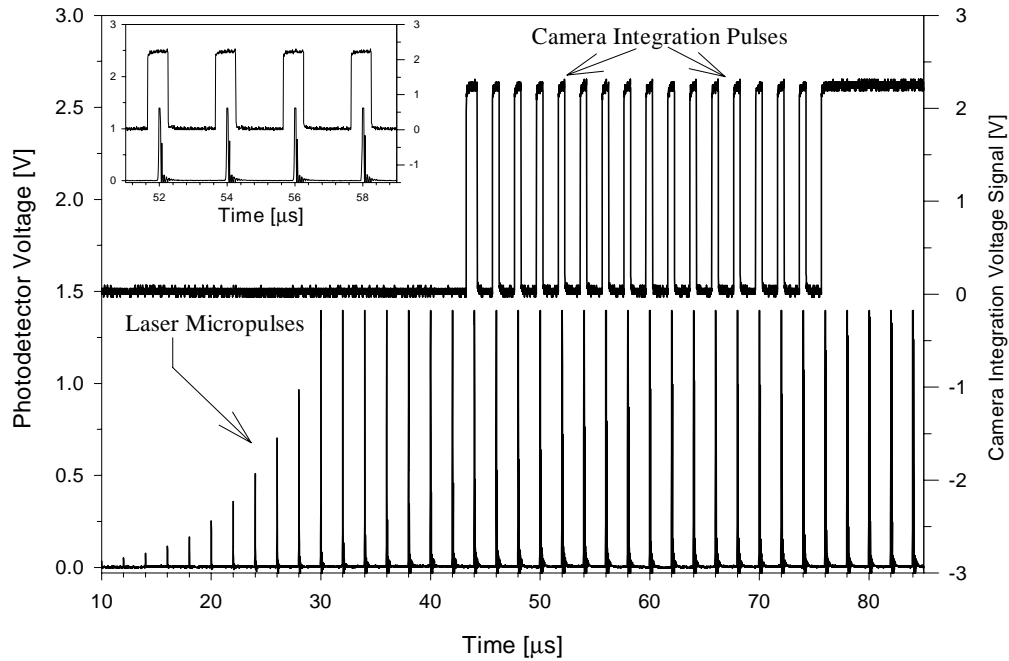


Figure 12. Oscilloscope traces of the photodetector output and camera integration output. The inset figure focuses on the time scale to show overlap. Traces were acquired simultaneously during the test shown in Figure 7.

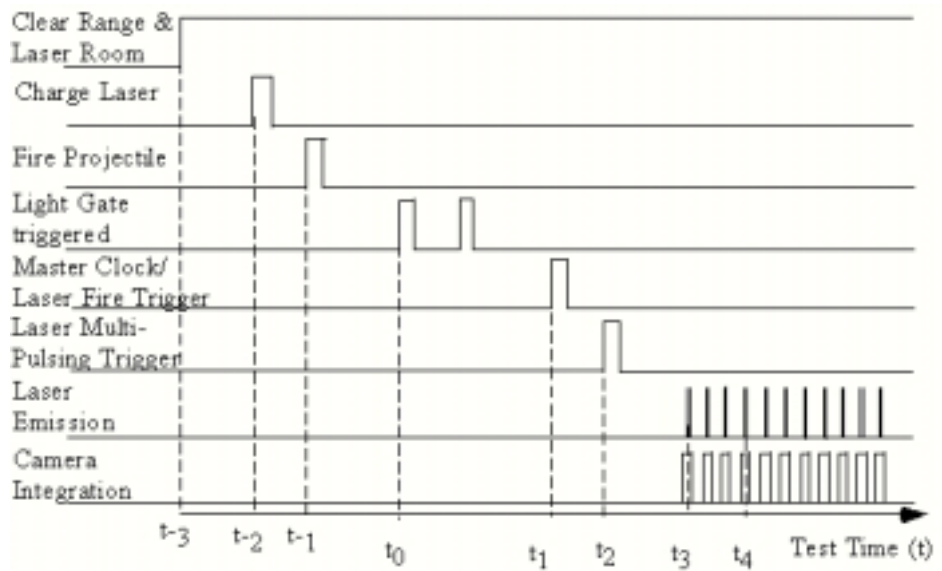


Figure 13. Timing diagram for the ballistic impact tests.

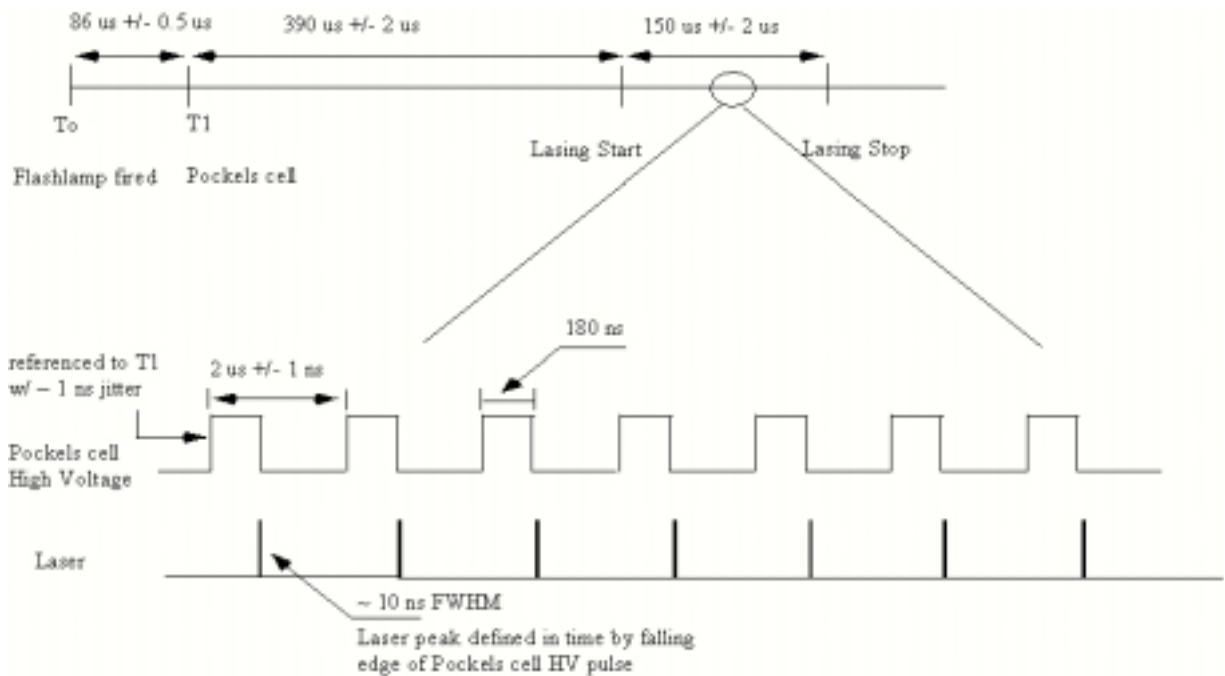


Figure 14. Timing diagram for the multiple Q-switching ruby laser.

and the laser time (from fire trigger to laser emission - see Figure 14). The light gate has the capability to measure the projectile speed in real time. Therefore, once properly calibrated, speed variations will not affect the test timing. The delay between t_1 and t_2 , t_3 is detailed in Figure 14. Time t_4 indicates projectile target impact.

Figure 14 shows a timing diagram of the ruby laser system. Note that capital letters used here define a time relative to the laser fire trigger (rather than the light gate trigger). The top line represents a chronological description of the laser macropulse. The bottom two lines show a chronological description of the lasing for a short number of pulses within the lasing envelope (macropulse). For these two lines, the Pockels cell line refers to the time dependent switching of the high voltage across the cell and the final line shows the laser pulses coincident with the closing of the high voltage on the Pockels cell.

Here time zero (T_0) is referenced to the firing of the flashlamps and time one (T_1) is referenced to the rise of the first Pockels cell high voltage pulse. Time one (T_1) was used for the laser reference time because the laser pulse is defined by the falling edge of the Pockels cell high voltage pulse⁸. All laser pulses can be referenced to the start of the Pockels cell pulsing with

high accuracy and precision. The camera is then slaved to this time as well.

Conclusions

A high-speed CCD camera has been successfully integrated with a high-speed ruby laser to acquire digital images at 500 kHz. Though not discussed in this paper, the camera and laser have individually been run at 1 MHz. Both the laser and the camera are commercially available products developed under the Small Business Innovative Research (SBIR) program with the Air Force Research Laboratory (AFRL/MNMF).

The required pulse energy for exposure was calculated according to the fluence requirements of the CCD array and the geometry of the experimental setup. Delivered pulse energy was measured at approximately 100 mJ/pulse. The dynamic range of the CCD array (12 bits) and the large energy range capability of the laser (3 orders of magnitude) allow for greater flexibility between delivered and calculated pulse energies in actual range tests. This facilitates application of the high-speed imaging system to a wide range of high-speed events.

This paper highlights the high-speed imaging capabilities of the Bay-10 gun range at the AFRL/MNMF. The high-speed ruby laser and high-frame rate

CCD camera were successfully integrated into real-time ballistic impact tests at 500 kHz. Currently, multiple cameras allow for stereoscopic imaging. These cameras exist and were in place for the tests reported herein. Stereoscopic imaging extends the system data reduction. In addition, the laser has the ability to generate holographic quality light at high repetition rates. Coupled with an in place high-speed holographic recorder, it provides Bay-10 with unparalleled imaging capability.

Future plans for this high speed imaging system include experiments on the fracture properties of safety glass and the dispersion of aerosols released from a storage canister during a destructive impact. It is also planned to extend the operation range of the system to 1 MHz and to fully explore operation with multiple time gates as well as mono and stereo imaging.

Acknowledgements

The authors would like to acknowledge the financial support of the U.S. Air Force through the Small Business Innovation Research Program. This invited paper is based on SPIE Paper 3968-06. The authors also acknowledge the contributions of Charles Goldey, Eugene Chennette, and Roger Hudson and of Continuum Electro-optics, James Norby, Jean-Marc Heritier, John Davis and Gurdaver Chahal.

References

1. Siegman, A.E., *Lasers*, University Science Books, Mill Valley, 1986.
2. Shaw, L.L., Steinmetz, L.L., Behrendt, W.C., Sonderman, J.B., Beer, G.K., Seppala, L.G., Romero, E., "A High-Speed, Eight-Frame Electro-Optic Camera with Multipulsed Ruby Laser Illuminator," 16th International Congress on High Speed Photography and Photonics, Strasburg, France, SPIE 491, 271-273, August 1984.
3. Shaw, L.L., Muelder, S.A., Rivera, A.T., Dunmire, J.L., Breithaupt, R.D., "Electro-Optic Frame Photography with Pulsed Ruby Illumination," 20th International Congress on High Speed Photography and Photonics, Victoria, B.C., September 1992. *Proc. SPIE* **1801**, 92-105 (1992).
4. Francis, C.L., "Enhanced Imagery through Laser Illumination," 1998 ITEA Test Instrumentation Workshop, 25-26 March 1998; available at <http://www.Edwards.af.mil/itea/paper98.htm> as "Paper 01."
5. Ellis, A.T., and Forney, M.E., "Application of a Ruby Laser to High-Speed Photography," *Proc. of IEEE* **51**(6), 1963.
6. Rowlands R.E., Taylor, C.E., and Daniel, I.M., "Ultrahigh-speed framing photography employing a multiply-pulsed ruby laser and a smear-type camera: application to dynamic photoelasticity," in *Proc. 8th Int. Conf. on High-Speed Photography* (June 1968).
7. Huntley, J. "High-Speed Laser Speckle Photography- Part I and II", *J. Opt. Eng.* **33**(5), 1994.
8. Goldey C.L., Grace, J.M., Nebolsine, P.E. , and Huntley, J.H., "Ruby laser repetitively pulsed at rates up to 500 kHz containing etalons and amplifications," in *Solid State Lasers VII, Proc. SPIE* 3265, pp. 144-154 (Jan. 1998).
9. Grace, J.M., Nebolsine, P.E., Goldey, C.L., Chahal, G., Norby, J., Hertitier, J-M. "Repetitively Pulsed Ruby Lasers as Light Sources for High-Speed Photography", *J. Opt. Eng.*, Vol. 37(8), Aug., 1998.
10. Grace, Jeffrey M.; Nebolsine, Peter E.; Snyder, Donald R.; Howard, Nathan E., and Long, J.R.; " Integration of a high-speed repetitively pulsed laser with a high-speed CCD camera," in *High-Speed Imaging and Sequence Analysis, Proc. SPIE Vol. 3642*, p. 133-141, (May 1999).
11. Grace, J.M., Nebolsine, P.E., Snyder, D.R., Chenette, E.R., "Dynamic Ballistic Impact Events Imaged at 500 kHz Using Laser-Based Image Acquisition," SPIE Paper 3968-06, 12th International Electronic Imaging Conference, High Speed Imaging II Session, San Jose, CA, 27 January 2000.
12. Wu, Pingfan, Lempert, Walter R., and Miles, Richard B., "Megahertz Pulse-Burst Laser and Visualization of Shock-Wave/Boundary-Layer Interaction," *AIAA Journal* **38**(4), 672ff. (2000).